

# Design of Operation Strategy for Canal Structures


Kazem Shahverdi<sup>1\*</sup>, Hassan Mollazeynali<sup>2</sup>, Safar Marofi<sup>3</sup>

1- Assistant Professor, Department of Water Science and Engineering, Faculty of Agriculture, Bu-Ali Sina University, Hamedan 65178-38695, Iran.

2- B.Sc. Student, Department of Water Science Engineering, Faculty of Agriculture, Bu-Ali Sina University, Hamedan, 65178-38695, Iran.

3- Professor, Department of Water Science and Engineering, Faculty of Agriculture, Bu-Ali Sina University, Hamedan 65178-38695, Iran.

\* [k.shahverdi@basu.ac.ir](mailto:k.shahverdi@basu.ac.ir)

Received: 4 August 2023, Accepted: 24 August 2023  J. Hydraul. Homepage: [www.jhyd.iha.ir](http://www.jhyd.iha.ir)

## Abstract

Simple operation strategies make the users capable of regulating standard gates, such as overshoot and undershot gates. For complicated operations, a control algorithm must be used, almost always done by programming the control algorithm within a programming software and coupling it with a canal simulator. In this research, a new operation strategy was designed to regulate inline water structures in the Alborz canal in Mazandaran province, Iran. To this end, the simple and common classic proportional integral derivative controller was coded in the rule boundary condition, being called by HEC-RAS 5.0.7 during the canal simulation. The HEC-RAS model of the canal was prepared designing a controller for each inline gate to regulate upstream water depth. Performance indicators and statistical indices were used for evaluation. The tuning of the controller results gains indicated that the proportional gain of  $k_p$  is 5, 4.5, 3.5, and 5 for regulating gates 1-4, respectively. The  $k_i$  integral gain and  $k_d$  derivative gain were also tuned. The results showed that the designed model can simultaneously simulate the canal and regulate the gates successfully, obtaining a maximum and average depth errors of 7.5% and about 1% which are quite acceptable. The adequacy was 1 in almost all cases, and the efficiency was more than 0.97 with equitable distribution.

**Keywords:** Automation, HEC-RAS, Tuning, Water Delivery and Control Structures.

© 2024 Iranian Hydraulic Association, Tehran, Iran.



This is an open access article distributed under the terms and conditions of the Creative Commons Attribution 4.0 International (CC BY 4.0 license) (<http://creativecommons.org/licenses/by/4.0/>)

## 1. Introduction

Canal networks have many hydraulic structures for different purposes. A hydraulic structure is a structure submerged or partially submerged in any body of water, which disrupts the natural flow of water. They can be used to divert, disrupt or completely stop the flow. The hydraulic characteristics of the sluice gates, as a simple and widely used structure, has been numerically and experimentally investigated in many researches (Daneshfaraz et al., 2022; Daneshfaraz et al., 2022; Daneshfaraz et al., 2023; Daneshfaraz et al., 2023). To simulate a canal network and its hydraulic structure, hydraulic models are used that play an essential role in simulating canals, rivers, reservoirs, various structures, etc. Some specialized hydraulic software that has been developed so far are the river analysis system developed by the hydrologic engineering center of the US Army Corps of engineers (HEC-RAS), storm water management model (SWMM), simulation of irrigation canals (SIC), the integrated software package for river, urban or rural management (SOBEK), irrigation canal system simulation (ICSS). Although these models solve the complete forms of the Saint-Venant Equations (SVE), some other simplified and approximated models have been developed based on SVE.

The simplification methods are explicit (Bonet et al., 2017), implicit methods with the Preissman scheme (Figueiredo et al., 2013), transformation methods (Hayami, 1951), the orthogonal collocation method (Dulhoste et al., 2004). Of the approximated models are Integrator Delay (ID) model (Weyer, 2008), the integrator resonance model (van Overloop, Horváth, & Aydin, 2014); the data-driven model based on neural networks, fuzzy systems, linear systems, and pattern search methods (Herrera et al., 2013; Tavares et al., 2013), etc. In Isapoor et al. (2011), simple downstream and local classic controllers were formulated in Sobek, and the results of performing the provided model were evaluated. In Shahdany et al. (2019), a centralized automatic control system was developed to improve canals operation increase as well as water delivery flexibility. Despite previous studies applying traditional water demand strategies, they applied both predictable and unpredictable water demands representing advanced operations. Hashemy et al. (2013) developed

another advanced controller based on a prediction strategy to improve the performance of the main canals while simulating the studied canal using Sobek. In Arauz et al. (2020), linear matrix inequalities was used to tune the classic controller gains to regulate the gates in the ASCE test case canal number 1, where the integrator delay model was applied in controlling steps and tested using Sobek.

Having the source code of the irrigation conveyance simulation system package, written in FORTRAN, it has been used in various forms combination with several controllers, e.g., a learning classifier was developed and added as a subroutine to the irrigation conveyance simulation system package (Shahverdi & Monem, 2015). The ant colony optimization model was linked with the irrigation conveyance simulation system package, as a subroutine, showing reasonable results in various operations including normal and water deficit conditions (Fateme et al., 2020). Almost all controllers and optimizers are provided in MATLAB and Python programming languages, making it difficult to be linked with the irrigation conveyance simulation system package.

Among various controllers, the classic proportional integral derivative is the simplest, fastest, and the most popular one implemented in several irrigation canals for the control purposes (Saddam and Battle, 2020; Zamani et al., 2015). Since its performance largely depends on the gains, several methods, such as auto-tune variation (Litrico et al., 2007), have been proposed to analytically tune them. Before implementing the classic controller in the actual canal, it should be tested as local upstream and distance downstream ways as done by Lozano et al. (2010). Of analytical ways to tune the controller is encapsulating the classic controller within a linear quadratic regulator feedback gain as done by Zhong et al. (2020). To this end, a simplified simulator of the canal was employed. In particular, an optimization procedure was followed to minimize the changes in water levels and flows, leading to satisfactory performance. Conde et al. (2021) reviewed both hydraulic models and employed controlled systems. Among the existing controllers, the classic controller (or its parts such as the proportional controller and the proportional integral controller) is more common due to its simplicity in formulation and robustness in controlling.

In control problems of hydraulic structures, a hydraulic model is usually embedded and coupled with a controller written often in MATLAB, FORTRAN, and Python that makes it difficult to run and perform by most operators and engineers, in practice, when manipulating gates for water delivery and distribution purposes. They either is not familiar with controllers or have not high-performance computers needed to run complicated models in water authorities often, especially in developing countries. However, water engineers are almost familiar with HEC-RAS as a free and user-friendly hydraulic model.

It is a practical hydraulic and widely used model in the field of water engineering. Defining geometrical and hydraulic models, it simulates steady and unsteady flows, and gradually-varied flow under subcritical, supercritical, and mixed flow conditions. It calculates water level along the canal by solving the energy equation with the standard step-by-step iterative method (Daneshfaraz et al., 2019). It has some built-in simple gate types, such as sluice, radial, and overflow gates, with related specific equations that are common facilities to regulate water level using a set of empirical equations. For a specific gate type needed to be simulated, a non-standard gate can be created with a series of rating curves named user defined curves, where each curve is associated with a specific gate opening. Two other control options are time series, where a gate opening is set by the user for each time step, and controlled elevation examined (Mollazeynali & shahverdi, 2022). In case of a more complex operation, in which the existing flow control device does not simply fit within the confines of the built-in gates, rules boundary condition can be used in HEC-RAS that has many advantages and is less known for users (Deshays et al., 2021; Goodell, 2014; Goodell, 2016; Leon & Goodell, 2016). Something that has not been investigated and implemented in the irrigation canals so far.

The objective of this research was to design an advanced operation strategy, which allows engineers to handle all flow control scheme possible regardless of having a high-performance computer or knowing coding programs, by developing the classic controller and embedding it in the rules boundary condition in HEC-RAS to regulate inline gates, which is robust model despite its simplicity. In this case, all computations are done in HEC-RAS 5.0.7 as a hydraulic model, and the

boundary conditions are calculated with the classic controller. The geometric and flow parameters of the Alborz canal, located at Mazandaran province in Iran, were gathered, and the Alborz canal model was prepared. Two operational scenarios were used to tune the classic controller gains, and two other scenarios were tested for evaluation purposes using standard indicators and statistical indices.

## 2. Methodology

### 2.1. Studied Canal

The Alborz irrigation and drainage network, located in Mazandaran province, covers 52752 hectares of agricultural lands of the Babolroud, Talar, and Siahroud river basins. This region is bounded by the Mazandaran Sea from the north, the Alborz Mountain from the south, the Siahroud River from the east, and the Babolroud river from the west. Its latitude is between  $36^{\circ} 15'$  and  $36^{\circ} 46'$ , and its longitude is between  $52^{\circ} 35'$  and  $53^{\circ} 00'$ . Its operation is done using a set of canals, drainages, and structures (16 turnouts and four regulating checks).

The main canal of the network is a concrete lining canal with a length of 12.6 km, which covers an agricultural area of about 40,973 hectares by drawing water from the Ganj-Afroz diversion dam. It is a trapezoidal canal with 1V:1.5H and has a bed slope of 0.0003 until the first regulating gate and 0.0002 in the rest of the canal. The bed width varies between 3.5 and 4 m. In this research, the geometric and flow parameters of the canal were gathered. The HEC-RAS model of the Alborz canal was prepared, and then, different operational scenarios were tested and evaluated. A schematic view of the Alborz canal along with its location is presented in Figure 1, where TO1-TO16 refer to turnouts and C1-C4 refer to regulating check gates.

### 2.2. Classic Controller

One of the simple and common control methods is the proportional integral derivative (PID) controller. It was used in many researches in industry and water engineering (Arauz et al., 2020; Carlucho et al., 2019). Having received the inputs and comparing them with the corresponding set point, the outputs (regulating gate openings in this research) is calculated by (Shahverdi et al., 2022).

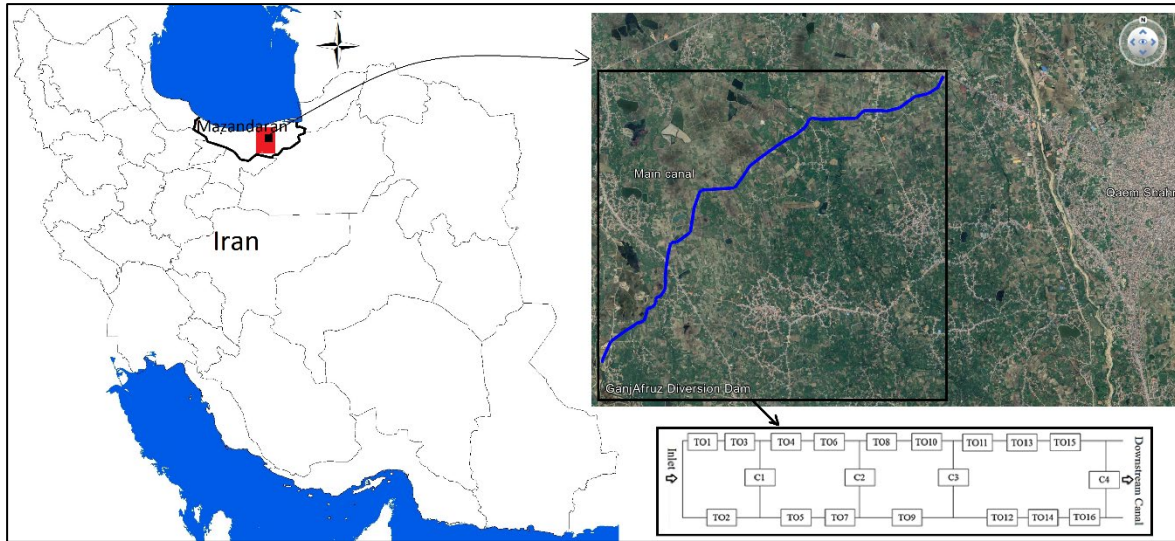


Fig. 1 Location of the studied area and schematic of the main canal.

$$u(kT) = u(kT - T) + k_p \left(1 + \frac{k_d}{T}\right) e(kT) - k_p \left(1 + \frac{2k_d}{T} - \frac{T}{k_i}\right) e(kT - T) + \frac{k_p k_d}{k_i} e(kT - 2T) \quad (1)$$

where  $u(kT)$  is the output that should be applied on the gate at the current time step;  $u(kT - T)$  is the gate opening at the previous time step;  $k_p$  is the proportional gain;  $k_d$  is the derivative gain;  $T$  is the time step chosen 30 s (0.0083 hr);  $e(kT)$  is the water depth error at the current time step;  $k_i$  is the integral gain;  $e(kT - T)$  is the water depth error at the previous time step;  $e(kT - 2T)$  is the water depth error at time step before previous time step.

### 2.3. Rules Boundary Condition

Various control algorithms have been developed and evaluated to control water-regulating structures in water conveyance and distribution canals. These algorithms should be coupled with a linear or non-linear simulator of canals to do the control action, resulting in a package, containing a controller and a simulator. In HEC-RAS, there is a boundary condition namely rules within which controllers' programming can be done. In this research, the simple classic controller code was written in the rule boundary condition to control water level regulating gates in the Alborz canal, and its performance was evaluated.

The rule operation boundary condition is applicable for in-line and lateral structures. As the rule operation boundary condition is opened for programming purposes, four distinguish boxes appear: description that any comments or

descriptions can be added; gate parameters that must be introduced, including the open/close rate of the gate that is under control and the maximum, minimum and initial openings of the gate; summary of variable initialization; and rule operations that includes two columns of row and operation. In the operation column, any supposed programs are written, and in each simulation time step, the written **commands** are performed from up to down.

In the rule boundary condition, there are several operators, including the comment, variable, simulation, operational, branch, math, and table operators. They are used to add texts, define the required variables and values, obtain the simulation value of the hydraulic variable during the simulation in a considered time and cross-section, apply adjustments to gates such as the gate height, write conditional orders like if-then-else, and extract information from the provided tables.

To describe the operators in details and implement the classical controller in the rule operation boundary condition, the classic controller code written in the rule boundary condition in the first reach of the Alborz canal to control the first regulating gate is shown in Figure 2. It should be noticed that separate codes should be written for each regulating structure, i.e., the developed controller is a decentralized one. Note also that in this way a hydraulic simulation is done, and there is no need to couple with another programming

language. Here, the gate openings are calculated based on the classic controller equations rather than the orifice or weir equation, meaning that

there is a gate whose opening is calculated using the classic controller. All other conditions are similar to gates.

row	Operation
1	! Used Variable
2	! Constant PID gain
3	Real 'Kp' (Initial Value = 5)
4	Real 'Ki' (Initial Value = 0.005)
5	Real 'Kd' (Initial Value = 0.0035)
6	! Simulation Values
7	! Water surface elevation in upstream- for e(KT)
8	'WS EL 0' = Cross Sections:WS Elevation(BABOL ROOD,ALBORZ,948.65,Value at previous time step)
9	! Water surface elevation in upstream- for e(KT-T)
10	'WS EL -1' = Cross Sections:WS Elevation(BABOL ROOD,ALBORZ,948.65,Value at specified lag,0.016666)
11	! Water surface elevation in upstream- for e(KT-2T)
12	'WS EL -2' = Cross Sections:WS Elevation(BABOL ROOD,ALBORZ,948.65,Value at specified lag,0.025)
13	! Gate opening (one step previous)
14	'u(KT-T)' = Inline Structures:Gate.Opening(BABOL ROOD,ALBORZ,948.61,Gate #1,Value at previous time step)
15	! PID values
16	! Coefficient in expansion 2
17	'K1' = ((1) + (120.48 * 'Kd')) * ('Kp')
18	! Coefficient in expansion 3
19	'K2' = (((1) + (240.96 * 'Kd')) - (0.0083 * 'Ki'^-1)) * (-1 * 'Kp')
20	! Coefficient in expansion 4
21	'K3' = ('Kd' / 'Ki') * 'Kp'
22	! Depth error (Current)
23	'e(KT)' = 'WS EL 0' - 102.665
24	! Depth error (One step previous)
25	'e(KT-T)' = 'WS EL -1' - 102.665
26	! Depth error (Two step previous)
27	'e(KT-2T)' = 'WS EL -2' - 102.665
28	! Operation
29	! Forming main expersions
30	'Expersion 1' = 'u(KT-T)'
31	'Expersion 2' = 'K1' * 'e(KT)'
32	'Expersion 3' = 'K2' * 'e(KT-T)'
33	'Expersion 4' = 'K3' * 'e(KT-2T)'
34	! Compute new gate opening
35	'u(KT)' = (('Expersion 1' + 'Expersion 2') + 'Expersion 3') + 'Expersion 4'
36	! Operational command
37	Gate.Opening(Gate #1) = 'u(KT)'
38	! End Of Operation

Fig. 2 Codes in rule operations to calculate the gate opening based on the classic controller.

The code in Figure 2 is explained according to the comments number and the operators used. Any line beginning with an exclamation mark corresponds to some explanations, and no calculation is done in these lines. Lines 3-5 encompass new variables assigned the values of classical gains  $k_p$ ,  $k_i$ , and  $k_d$  as 5, 0.05, and 0.0035, respectively. These values are constant during the simulations done in each scenario. They were determined by trial and error. In lines 8, 10, 12, and 14, the get simulation value operator was used corresponding to the water surface elevation of the nearest cross-section located upstream of the regulating gate at one time step, two time step, and three time step before the current time step, respectively. The nearest cross-section distance from the regulating structure is 0.5 m.

The values of  $k_1$ ,  $k_2$ , and  $k_3$  are calculated based on the constants  $k_p$ ,  $k_i$ ,  $k_d$ , and  $T$  at lines

17, 19, and 21, respectively. The water depth errors are calculated in lines 23, 25, and 27 considering set points that are 3.6, 3.2, 2.8, and 2.5 m in reaches 1-4, respectively. The number 102.665 in Figure 2 is the water surface elevation that corresponds to the set point of 3.6 m in the first reach. Finally, the components of equation 1 are calculated in lines 30-33, and  $u(kT)$  is calculated in line 35. All calculations are based on the math operator in the rule operation boundary condition. In line 37, the final output is a set operational parameter operator applied to the gate as a new adjustment of the gate.

It should be noted that the minimum and maximum openings of regulating gates were considered as 0.1 and 2.4 m based on the real field data received, respectively. The initial openings of the regulating gates were 1.05, 1.40, 1.67, and 1.79 m in reaches 1-4,

respectively. It should be also noted he data were received from the water office of Mazandaran regional water company.

## 2.4. Tuning and validation

Two operational scenarios (S1 and S2), were selected to tune classic controller gains and evaluate the performance of the rule operation boundary condition and related classic controller, and two other operational scenarios (S3 and S4) were selected for validation purposes (Table 1). The initial conditions in both tuning and validation phases were considered as the inflow of 15.5 m<sup>3</sup>/s, all turnouts are closed, and the target depths upstream of the regulating gates of 1-4 are 3.6, 3.2, 2.8, and 2.5 m, respectively.

S1 and S2 are two consecutive scenarios with respectively increases and decreases at the canal inlet, meaning the inflow to the canal was increased to 22.353 m<sup>3</sup>/s from 15.5 m<sup>3</sup>/s in S1 delivered 24 hr. In S2, the initial inflow of 15.5 m<sup>3</sup>/s was decreased to 12.8 m<sup>3</sup>/s delivered 12 hr, and then, it was decreased to 9 m<sup>3</sup>/s from 12.8 m<sup>3</sup>/s delivered 6 hr, and finally, increased to 12.8 m<sup>3</sup>/s again delivered 6 hr. In both S3 and S4, the initial inflow was 15.5 m<sup>3</sup>/s decreased to 8.8 m<sup>3</sup>/s and 6 m<sup>3</sup>/s, respectively. The flow changes in turnouts are underlined in Table 1. It should be noticed that these scenarios were defined based on the data received from the water office of Mazandaran regional water company.

**Table 1.** Data used for the tuning and validation of the controller gains (m<sup>3</sup>/s).

	Tuning				Validation	
	S1	S2		S3	S4	
	Time (0-24 hr)	Time (24-36 hr)	Time (36-42 hr)	Time (42-48 hr)	Time (0-24 hr)	Time (24-48 hr)
Head	22.353	12.8	9	12.8	8.8	6
TO1	0.25	0.25	0.25	0.25	0	0
TO2	1.4	1.4	<u>1</u>	<u>1.4</u>	0.3	0.3
TO3	1.7	1.7	<u>1.2</u>	<u>1.7</u>	<u>2</u>	<u>1.4</u>
TO4	0.01	0.01	0.01	0.01	0	0
TO5	0.015	0.015	0.015	0.015	0.03	0.03
TO6	0.012	0.012	0.012	0.012	0	0
TO7	0.047	0.047	0.047	0.047	0.12	0.12
TO8	0.01	0.01	0.01	0.01	0	0
TO9	0.01	0.01	0.01	0.01	0	0
TO10	2.7	2.7	<u>1.9</u>	<u>2.7</u>	<u>2.8</u>	<u>2</u>
TO11	0.057	0.057	0.057	0.057	0	0
TO12	0.019	0.019	0.019	0.019	0	0
TO13	0.057	0.057	0.057	0.057	0	0
TO14	0.046	0.046	0.046	0.046	0.21	0.21
TO15	0.02	0.02	0.02	0.02	0	0
TO16	0.5	0.5	<u>0.35</u>	<u>0.5</u>	<u>1</u>	<u>0.7</u>
Downstream	15.5	5.947	3.997	5.947	2.34	1.24

To obtain the appropriate values of classic controller gains, the proportional gain was first found out by trial and error for each regulating gate. The appropriate values are those values that lead to the employed indicators being closer to the associated desired values.  $k_p$  values of 0.5, 1.5, 2.5, 3.5, 4.5, and 5 were tested for each regulating gate separately. Having determined  $k_p$  values in all reaches, the appropriate values of  $k_i$  in all reaches were secondly considered. To this end, the range of 0.0001-0.05 were

tested. Finally,  $k_d$  values were determined supposing the range of 0.0001-0.01. The procedure of finding the gains was from the first to the last regulating gates. For example, in the case of  $k_p$ , its appropriate value for the first regulating gate was determined by testing the considered bound, while there were no changes in the rest of the regulating gates. The appropriate value for the second regulating gate was determined by testing the considered bound, while there were no changes in the third

and fourth regulating gates and the first regulating gate was controlled with the proportional controller using determined  $k_p$  gain. This procedure was used in finding  $k_i$  and  $k_d$  values as well.

## 2.5. Evaluation indicators

Two standard indicators of maximum absolute error (MAE) and integral absolute error (IAE) along with two statistical indices of root mean square error (RMSE) and scatter index (SI) were used to evaluate the developed model performance defined respectively as (Daneshfaraz et al., 2022).

$$MAE = \frac{\max(|Y_{target} - Y|)}{Y_{target}} \quad (2)$$

$$IAE = \frac{\sum_{T=0}^D (|Y_{target} - Y|)}{Y_{target}} \quad (3)$$

$$RMSE = \sqrt{\frac{1}{n} \sum (x_i - y_i)^2} \quad (4)$$

$$SI = \frac{RMSE}{\bar{x}} \quad (5)$$

where  $Y_{target}$  is the set point,  $Y$  is depth,  $T$  is the time step,  $D$  is total simulation time,  $x_i$  is observed data,  $y_i$  is simulated data,  $n$  is the total number of data, and  $\bar{x}$  is the average of the observed data.

Maximum absolute error indicator shows the maximum deviation of the depth from the associated set point during the simulation, and the integral absolute error indicator shows the average deviation from the associated set point during the simulation. Their ideal values of are zero (Shahverdi & Monem, 2012). Lower root RMSE shows better performance (Fard et al., 2021). The ideal value of scatter index is less than 0.3 (Howard et al., 2009).

To assess the flow distribution, water distribution indicators, including adequacy, efficiency, equity, and dependability were used. In this research, water distribution performance was conducted using indicators Adequacy ( $MPA$ ), Efficiency ( $MPF$ ), defined respectively by equations (6-7), Equity ( $MPE$ ), and Dependability ( $MPD$ ) presented by Molden and Gates (1990).

$$MPA = \frac{1}{T} \sum_{\Delta t} \left[ \frac{1}{N} \sum_N \left( \frac{Q_d}{Q_r} \right) \right] \quad \text{if } Q_d \leq Q_r \quad (6)$$

$$\text{otherwise } \frac{Q_d}{Q_r} = 1$$

$$MPF = \frac{1}{T} \sum_{\Delta t} \left[ \frac{1}{N} \sum_N \left( \frac{Q_r}{Q_d} \right) \right] \quad \text{if } Q_r \leq Q_d \quad (7)$$

$$\text{otherwise } \frac{Q_r}{Q_d} = 1$$

where  $N$  is number of turnouts;  $Q_d$  is delivered discharge;  $Q_r$  is requested discharge;  $Cv_N$  is coefficient of spatial variation of discharge;  $Cv_T$  is coefficient of temporal variation of discharge;  $Y_{target}$  is target depth upstream the check structure;  $y$  is water level at each time step;  $\Delta t$  is simulation time step;  $T_{dur}$  is total simulation time; and  $T$  is number of time steps in a total simulation period, defined as  $T = T_{dur} / \Delta t$ .

## 3. Results and Discussion

As presented, different values of  $k_p$ ,  $k_i$ , and  $k_d$  were used to tuning them. Based on the investigations done, the  $k_p$ ,  $k_i$ , and  $k_d$  gains had a more sensible effect on the maximum and average errors, and  $RMSE$  indicators, respectively. Hence, the maximum error was chosen as the best indicator to find suitable  $k_p$ . Since the average error shows the average deviations of water depth from the set point, it was chosen to find suitable  $k_i$ . Also,  $RMSE$  was used to find out  $k_d$ . It should be noticed that these indicators have similar behavior in general; however, some trivial changes may exist in some cases. The results of finding the controller gains in the regulating gates is shown in Figure 3. Their final appropriate values are given in Table 2. After determining the controller gains for all regulating gates, the model was run for 48 hr while applying the proportional controller, the proportional integral controller, and the proportional integral derivative controller. It should be mentioned that the  $k_p$  gain is the only gain that is used in the proportional controller. However, the  $k_p$  and  $k_i$  gains are used in the proportional integral controller, and all gains  $k_p$ ,  $k_i$ , and  $k_d$  are used in the proportional integral derivative controller. The results of depth deviations from

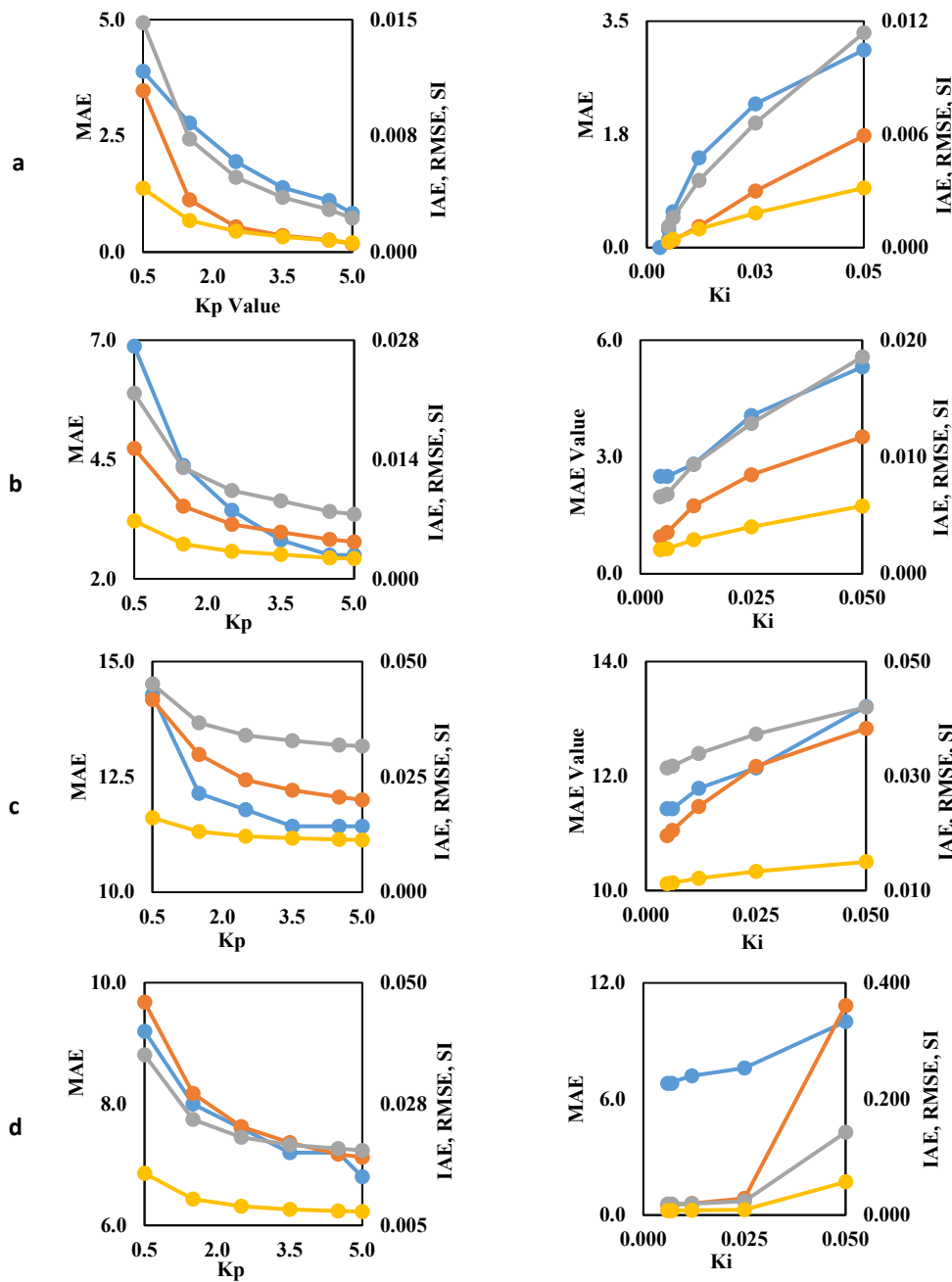


Fig. 3 Results of indicators to tuning the controller gains in the regulating gates, (a) regulating gate 1, (b) regulating gate 2, (c) regulating gate 3, and (d) regulating gate 4.

the associated set points upstream of each regulating gate is shown in Figure 4. As shown, the indicator curves associated with  $k_p$  represent a similar behavior in all regulating gates. All indicators almost uniformly decrease with increasing  $k_p$ . Since the proportional controller with the gain of  $k_p$  is the most important in the classic controller and more sensitive to the maximum error, the maximum error variation was considered to find suitable  $k_p$ , leading to  $k_p$  was obtained to 5, 4.5, 3.5,

and 5 (as shown in Table 2) with the maximum error of 0.28%, 2.5%, 11.08%, and 6.8% for regulating gates 1-4, respectively. As seen, maximum errors are reasonable and applicable in practice. Turnouts 8-10 are located upstream of regulating gate 3, and turnout 10 delivers much more flow compared to the other turnouts which cause maximum error in the third reach to be relatively greater than the other regulating gates.



**Table 2.** Obtained the classic controller gains and performance indicators.

Regulating gate	Controller gains	MAE (%)	IAE (%)	RMSE	SI
1	$k_p=5.0$	0.28	0.0002	0.0009	0.0003
	$k_i=0.005$				
	$k_d=0.0035$				
2	$k_p=4.5$	2.50	0.0027	0.0063	0.0020
	$k_i=0.0045$				
	$k_d=0.004$				
3	$k_p=3.5$	11.07	0.0187	0.0310	0.0111
	$k_i=0.0048$				
	$k_d=0.003$				
4	$k_p=5.0$	6.80	0.0167	0.0187	0.0075
	$k_i=0.007$				
	$k_d=0.0015$				

Regarding  $k_i$  gain, the indicators increase with increasing  $k_i$  from 0.0001 to 0.05 in general. The appropriate  $k_i$  obtained for the regulating gates 1-4 are 0.005, 0.0045, 0.0048, and 0.007 with average error of 0.0002, 0.0027, 0.0187, and 0.0167%, respectively. As shown, the mean deviations from set points are very little, leading to the proportional controller being capable to reduce the deviations successfully. According to the depth errors figures, the errors are reduced in all regulating gates as an integral part, i.e.,  $k_i$ , is added to the proportional integral controller and comprised of the proportional integral controller. This reduction shows the successful effect of the  $k_i$  on the water depth variation. It should be noticed that the integral part effect in the regulating gates 1 and 2 is much more than those of regulating gates 3 and 4. As mentioned before, a large discharge happens in turnout 8 upstream of reach 3, causing large variations in depth during the simulation time and greater average error.

The derivative part of the classic controller is related to the little fluctuations in water depth. The classic controller in the Alborz canal is too sensitive to the derivative part and its coefficient, i.e.,  $k_d$ , caused the water depth fluctuations to be improved in just a few values in reaches 1 and 2 and just one value in reaches 3 and 4. However, its effect in reducing water depth deviations is remarkable. Choosing the appropriate values of  $k_d$  in different reaches were done based on the RMSE indicator. Its lower value gives better performance. There were just one or two values of  $k_d$  with acceptable performance, resulted in charts with

one point or a straight line; therefore, its graphs were not shown in the figure. According to the results, it can result in control algorithms could directly be substituted in the rule operation as is used as a boundary condition in HEC-RAS, and the whole system is solved as a hydraulic problem.

After tuning the classic controller gains using two scenarios 1 and 2 in the Alborz canal, two other scenarios were chosen to test the designed the classic controller in HEC-RAS during 24 hr operation. The initial conditions were those values used in the tuning, and the operational condition was given in Table 1. The results of depth error after applying the changes in the reaches in S3 and S4 are respectively given in Fig. 5 and Fig. 6 and the corresponding indicators is given in Table 3.

As shown, all maximum errors are less than 7.5% and a few minutes were needed for the water depths to be established at the associated set points by the classic controller. The mean deviation from set points is too little according to the average errors that are less than 0.0399%. The ideal value of the SI indicator is less than 0.3. All the obtained SI values are less than 0.3. Therefore, the designed model with the classic controller has successful performance in terms of depth criteria.

The flow changes error during the flow delivery to turnouts in S1, as an example, is shown in Fig. 7. As shown, the maximum and minimum flow delivery errors are 0.02 and -0.02 m<sup>3</sup>/s, respectively, occurred during the first three hours. After that, the flow was almost established at the corresponding target value,

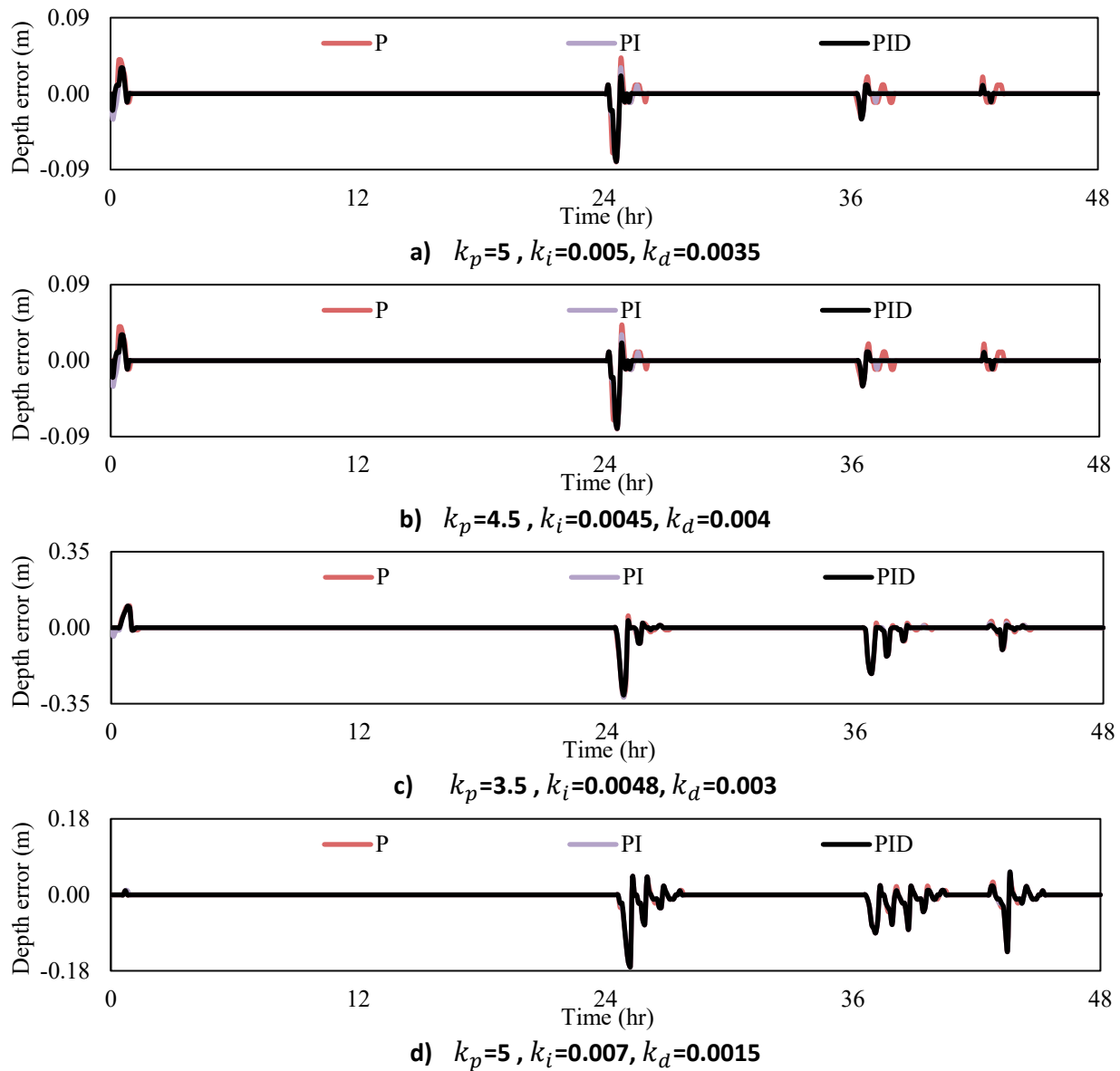


**Fig. 4** Depth errors upstream of regulating gates 1-4 represented respectively in a-d, while applying the final gains.

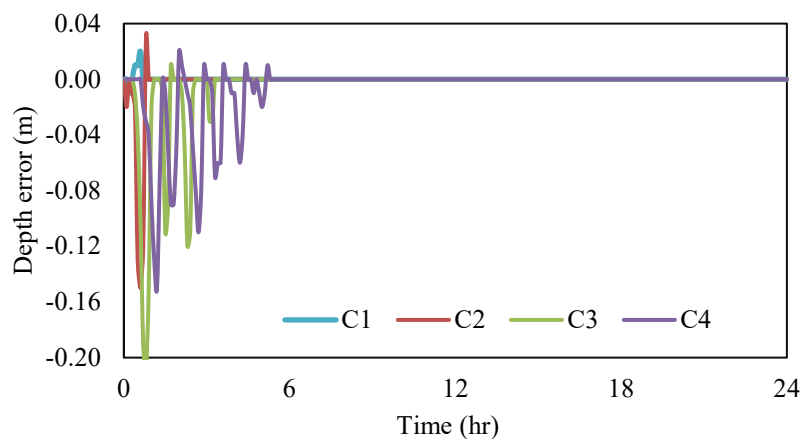


**Fig. 5** Depth error upstream of regulating gates in S3 based on the obtained gains.

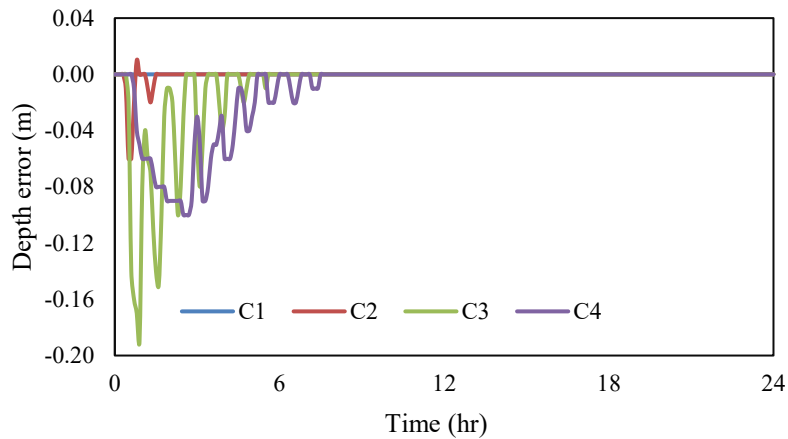


Fig. 6 Depth error upstream of regulating gates in S4 based on the obtained gains.

Table 3. Performance indicators of the controller in S3 and S4 based on the obtained gains.

Regulating gate	S3				S4			
	MAE (%)	IAE (%)	RMSE	SI	MAE (%)	IAE (%)	RMSE	SI
1	0.56	0.0005	0.0017	0.0005	0.00	0.0000	0.0000	0.0000
2	4.69	0.0052	0.0152	0.0047	1.88	0.0022	0.0059	0.0018
3	7.50	0.0161	0.0263	0.0094	6.79	0.0260	0.0308	0.0110
4	6.00	0.0229	0.0228	0.0091	4.00	0.0399	0.0286	0.0114

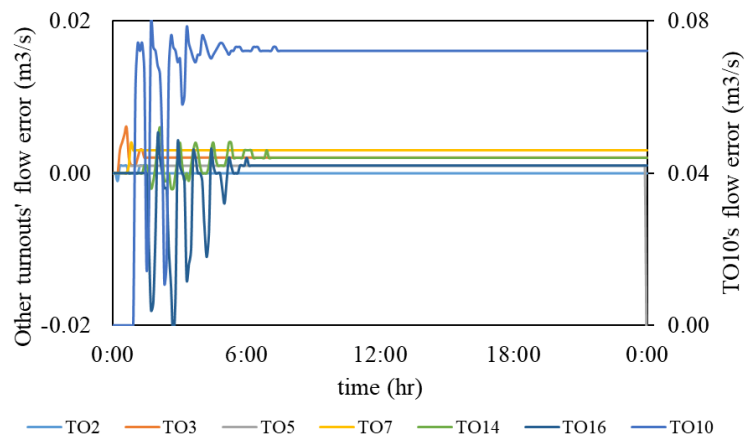


Fig. 7 flow changes' error during flow delivery to turnouts in S1.

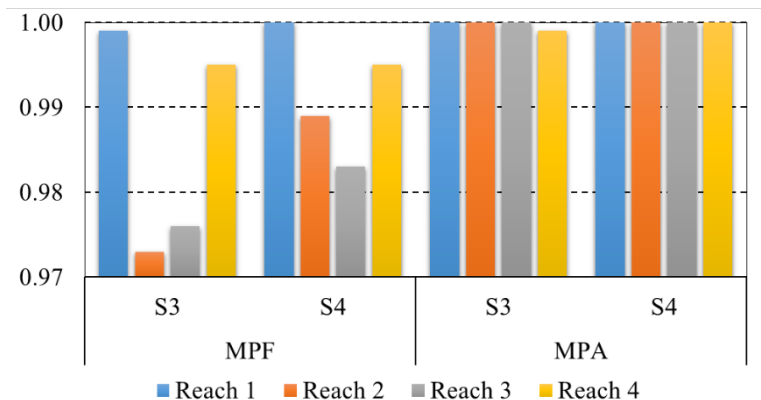


Fig. 8 Adequacy and efficiency indicators.

and the difference between requested and delivered flows have become zero, leading to an accurate water delivery.

In Fig. 8, the water distributions of adequacy and efficiency indicators in reaches 1-4 were presented, showing reasonable results since the adequacy values are all 1 except for reach 4 in S3, which is a bit smaller than 1. Note that the ideal values of the efficiency and adequacy indicators are 1. Regarding the efficiency indicator, they are all greater than 0.97 and too close to the corresponding ideal value. The equity in S3 and S4 were respectively obtained as 0.014 and 0.008, showing the water is distributed equitably. The dependability values were 0.003 and 0.008 in S3 and S4, respectively. The ideal value of these indicators is zero.

An advantage of such a model in which a controller is embedded within a hydraulic model rather than a hydraulic model is embedded within a controller is that most of the operators and engineers managing water delivery and distribution systems are not familiar with complicated coupled models, but they all familiar with HEC-RAS as a free and user-friendly hydraulic model. Therefore, providing an HEC-RAS model where a robust controller regulates gates can be more efficient and interesting, causing they support and use such models. In addition, high-performance computers are needed to run complicated control models that are not available to water authorities often, at least in developing countries.

#### 4. Notation

$Cv_N$	coefficient of spatial variation of discharge
$Cv_T$	coefficient of temporal variation of discharge
$e(kT)$	water depth error at the current time step
$e(kT - 2T)$	water depth error at penultimate time step
$IAE$	integral absolute error
$k_d$	derivative gain
$k_i$	integral gain
$k_p$	proportional gain
$MAE$	maximum absolute error
$MPA$	Adequacy indicator
$MPD$	Dependability indicator
$MPE$	Equity indicator
$MPF$	Efficiency indicator
$N$	number of turnouts

$PID$	proportional integral derivative
$Q_d$	delivered discharge
$Q_r$	requested discharge
$RMSE$	Root Mean Square Error
$S1$	operational scenario 1
$S2$	operational scenario 2
$S3$	operational scenario 3
$S4$	operational scenario 4
$SI$	scatter index
$T$	time step
$T_{dur}$	total simulation time
$u(kT)$	gate at the current time step
$u(kT - T)$	gate opening at the previous time step
$y$	water level at each time step
$y_{target}$	target depth

#### 5. Conclusion

In this research, a new aspect of controlling in-line regulating gates was introduced. The classic controller as a water level controller was programmed in the rule operation boundary condition in HEC-RAS and used instead of the usual orifice equation to calculate gate openings. After gathering hydraulic and geometric data on the Alborz canal, providing an HEC-RAS model of the canal, and programming the classic controller in the rule operation boundary condition, the classic controller gains were determined using operational scenarios.  $k_p$  gains, as the most essential and effective gain, were obtained 5, 4.5, 3.5, and 5 in reach 1-4, respectively. The provided model was tested using two operational scenarios, leading to satisfactory results. The results analysis showed that adding the  $k_i$  gain causes the mead deviation from the set points to be reduced and adding the  $k_d$  gain causes little fluctuations to be removed. The maximum and average depth errors were reasonable. The adequacy was obtained as 1 in almost all cases. The efficiency was more than 0.97 with equitable distribution. According to the results, it could be concluded that the rule operation boundary condition is a good choice to formulate a controller algorithm to adjust regulating gates. This work was the first one in this regard. However, formulating complex controllers should be investigated in future studies.

#### 6. References

Arauz, T., Maestre, J.M., Tian, X. & Guan, G. (2020). Design of PI controllers for irrigation canals

- based on linear matrix inequalities. *Water*, 12(3), 855, <https://doi.org/10.3390/w12030855>.
- Bonet, E., Gómez, M., Yubero, M. & Fernández-Francos, J. (2017). GOROSOBO: an overall control diagram to improve the efficiency of water transport systems in real time. *Journal of Hydroinformatics*, 19(3), 364-384.
- Carlucho, I., De Paula, M. & Acosta, G.G. (2019). Double Q-PID algorithm for mobile robot control. *Expert Systems with Applications*, 137, 292-307.
- Conde, G., Quijano, N. & Ocampo-Martinez, C. (2021). Modeling and control in open-channel irrigation systems: A review. *Annual Reviews in Control*, 51, 153-171.
- Daneshfaraz, R., Dasineh, M. & Ghaderi, A. (2019). Evaluation of Scour Depth around Bridge Piers with HEC-RAS (Case study: Bridge of Simineh Rood, Miandoab, Iran). *Environment and Water Engineering*, 5(2), 91-102.
- Daneshfaraz, R., Norouzi, R., Abbaszadeh, H. & Azamathulla, H.M. (2022). Theoretical and experimental analysis of applicability of sill with different widths on the gate discharge coefficients. *Water Supply*, 22(10), 7767-7781.
- Daneshfaraz, R., Norouzi, R. & Ebadzadeh, P. (2022). Experimental and numerical study of sluice gate flow pattern with non-suppressed sill and its effect on discharge coefficient in free-flow conditions. *Journal of Hydraulic Structures*, 8(1), 1-20.
- Daneshfaraz, R., Norouzi, R., Ebadzadeh, P. & Kuriqi, A. (2023). Influence of sill integration in labyrinth sluice gate hydraulic performance. *Innovative Infrastructure Solutions*, 8(4), 118.
- Daneshfaraz, R., Norouzi, R., Ebadzadeh, P., Di Francesco, S. & Abraham, J.P. (2023). Experimental study of geometric shape and size of sill effects on the hydraulic performance of sluice gates. *Water*, 15(2), 314, <https://doi.org/10.3390/w15020314>.
- Deshays, R., Segovia, P. & Duviella, E. (2021). Design of a MATLAB HEC-RAS Interface to Test Advanced Control Strategies on Water Systems. *Water*, 13(6), 763, <https://doi.org/10.3390/w13060763>.
- Dulhoste, J.-F., Georges, D. & Besançon, G. (2004). Nonlinear control of open-channel water flow based on collocation control model. *Journal of Hydraulic Engineering*, 130(3), 254-266.
- Fard, A.A., Shahdany, S.M.H., & Javadi, S. (2021). Automatic surface water distribution systems: A reliable alternative for energy conservation in agricultural section. *Sustainable Energy Technologies and Assessments*, 45, 101216, <https://doi.org/10.1016/j.seta.2021.101216>.
- Fatemeh, O., Hesam, G. & Shahverdi, K. (2020). Comparing Fuzzy SARSA Learning (FSL) and Ant Colony Optimization (ACO) Algorithms in Water Delivery Scheduling under Water Shortage Conditions. *Journal of Irrigation and Drainage Engineering*, 146(9), 04020028, [https://doi.org/10.1061/\(ASCE\)IR.1943-4774.0001496](https://doi.org/10.1061/(ASCE)IR.1943-4774.0001496).
- Figueiredo, J., Botto, M. A. & Rijo, M. (2013). SCADA system with predictive controller applied to irrigation canals. *Control Engineering Practice*, 21(6), 870-886.
- Goodell, C. (2014). Breaking the HEC-RAS Code: A User's Guide to Automating HEC-RAS. h2ls, 278p.
- Goodell, C. (2016). Advanced Gate Operation Strategies in HEC-RAS 5.0, doi:10.15142/T3430628160853.
- Hashemy, S., Monem, M., Maestre, J. & Van Overloop, P. (2013). Application of an In-Line Storage Strategy to Improve the Operational Performance of Main Irrigation Canals Using Model Predictive Control. *Journal of Irrigation and Drainage Engineering*, 139(8), 635-644.
- Hayami, S. (1951). On the propagation of flood waves. Disaster Prevention Research Institute, Kyoto University. Bulletin No. 1, Kyoto, Japan.
- Herrera, J., Ibeas, A. & de la Sen, M. (2013). Identification and control of integrative MIMO systems using pattern search algorithms: An application to irrigation channels. *Engineering Applications of Artificial Intelligence*, 26(1), 334-346.
- Howard, K., Zarillo, G., Splitt, M., Lazarus, S., Chiao, S., Santos, P. & Sharp, D. (2009). The impact of atmospheric model resolution on a coupled wind/wave forecast system. Preprints, 16th Conf. on Air-Sea Interaction, Phoenix, AZ, Amer. Meteor. Soc, CD-ROM P9.2.
- Isapoor, S., Montazar, A., Van Overloop, P. & Van De Giesen, N. (2011). Designing and evaluating control systems of the Dez main canal. *Irrigation and Drainage*, 60(1), 70-79.

- Leon, A.S. & Goodell, C. (2016). Controlling Hec-Ras using Matlab. *Environmental Modelling & Software*, 84, 339-348.
- Litrico, X., Malaterre, P.-O., Baume, J.-P., Vion, P.-Y. & Ribot-Bruno, J. (2007). Automatic tuning of PI controllers for an irrigation canal pool. *Journal of Irrigation and Drainage Engineering*, 133(1), 27-37.
- Lozano, D., Arranja, C., Rijo, M. & Mateos, L. (2010). Simulation of automatic control of an irrigation canal. *Agricultural Water Management*, 97(1), 91-100.
- Molden, D.J. & Gates, T.K. (1990). Performance measures for evaluation of irrigation-water-delivery systems. *Journal of Irrigation and Drainage Engineering*, 116(6), 804-823.
- Mollazeynali, H. & Shahverdi, K. (2022). Application and Evaluation of Elevation Controlled Gates Boundary Condition in HEC-RAS in Water Conveyance and Distribution Systems. *Journal of Water and Irrigation Management*, 12(4), 847-858. (In Persian)
- Saddam, G. & Battle, V.F. (2020). Robust Fractional Order Control of a Pool of a Main Irrigation Canal in Submerged Flow Condition. *IFAC-Papers OnLine*, 53(2), 16611-16616.
- Shahdany, S.H., Taghvaeian, S., Maestre, J. & Firoozfar, A. (2019). Developing a centralized automatic control system to increase flexibility of water delivery within predictable and unpredictable irrigation water demands. *Computers and Electronics in Agriculture*, 163, 104862, <https://doi.org/10.1016/j.compag.2019.104862>.
- Shahverdi, K., Alamiyan-Harandi, F. & Maestre, J. (2022). Double Q-PI architecture for smart model-free control of canals. *Computers and Electronics in Agriculture*, 197, 106940, <https://doi.org/10.1016/j.compag.2022.106940>.
- Shahverdi, K. & Monem, M.J. (2012). Construction and evaluation of the bival automatic control system for irrigation canals in a laboratory flume. *Irrigation and Drainage*, 61(2), 201-207.
- Shahverdi, K. & Monem, M.J. (2015). Application of reinforcement learning algorithm for automation of canal structures. *Irrigation and Drainage*, 64(1), 77-84.
- Tavares, I., Borges, J., Mendes, M.J. & Botto, M.A. (2013). Assessment of data-driven modeling strategies for water delivery canals. *Neural Computing and Applications*, 23(3), 625-633.
- Van Overloop, P.-J., Horváth, K. & Aydin, B.E. (2014). Model predictive control based on an integrator resonance model applied to an open water channel. *Control Engineering Practice*, 27, 54-60.
- Weyer, E. (2008). Control of irrigation channels. *IEEE Transactions on Control Systems Technology*, 16(4), 664-675.
- Zamani, S., Parvaresh Rizi, A. & Isapoor, S. (2015). The effect of design parameters of an irrigation canal on tuning of coefficients and performance of a PI controller. *Irrigation and Drainage*, 64(4), 519-534.
- Zhong, K., Guan, G., Tian, X., Maestre, J.M. & Mao, Z. (2020). Evaluating optimization objectives in linear quadratic control applied to open canal automation. *Journal of Water Resources Planning and Management*, 146(11), 04020087, [https://doi.org/10.1061/\(ASCE\)WR.1943-5452.0001286](https://doi.org/10.1061/(ASCE)WR.1943-5452.0001286).